Behavioral/Systems/Cognitive

Asymmetrical Modes of Visual Bottom-Up and Top-Down Integration in the Thalamic Nucleus Rotundus of Pigeons

Kristian Folta,[1] **Bettina Diekamp,**[2] **and Onur Güntürkün**[1]

[1]Institute for Cognitive Neuroscience, Department of Biopsychology, Faculty of Psychology, Ruhr-University Bochum, D-44780 Bochum, Germany, and [2]Department of Psychological and Brain Sciences, Johns Hopkins University, Baltimore, Maryland 21218

The aim of this study was to separate bottom-up and top-down influences within cerebral asymmetries. This was studied in the lateralized visual system of pigeons by recording from single units of the left and right diencephalic nucleus rotundus of the tectofugal pathway while visually stimulating the ipsilateral and/or contralateral eye. Analyses of response latencies revealed rotundal neurons with short and/or late response components. Cells with short latencies very likely represent bottom-up neurons participating in the ascending retinotectorotundal system. Because lidocaine injections into the visual Wulst produced a significant reduction of late response components only, neurons with long latencies were probably activated via a top-down telencephalotectorotundal system. The distribution and response characteristics of bottom-up and top-down neurons provided insight into several asymmetries of ascending and descending pathways. Asymmetries of the ascending retinotectorotundal system (bottom-up) were characterized by longer periods of tonic activation in the left and shorter response latencies in the right rotundus. Left-right differences in these responses probably facilitate faster access to visual input to the right hemisphere and a prolonged processing of this input in the left. The descending telencephalotectorotundal system (top-down) revealed a completely different lateralized organization. This system was characterized by long latency responses that exclusively derived from the left hemisphere, regardless of whether recordings took place in the left or the right rotundus. We assume that asymmetrical modes of visual processing within both hemispheres of the ascending tectofugal system are ultimately directed to left hemispheric forebrain mechanisms that subsequently generate executive control over sensory and motor structures.

Key words: **lateralization; birds; rotundus; visual system; tectofugal system; thalamofugal system**

Introduction

The human brain is lateralized, as are the brains of various nonhuman animals (Rogers and Andrew, 2002). Animal models should help to determine whether functional asymmetries result from bottom-up lateralizations of ascending sensory systems that shape associative forebrain processing, or whether they primarily emerge from top-down projections of forebrain structures that impose an asymmetrical control over sensory and motor systems. This is an integral question about the principal organization of cerebral asymmetries, and presently we are not aware of a single study that has approached it. Because the visual system of birds is highly lateralized with a superiority of the right eye–left hemisphere for object discriminations (Güntürkün, 2002), and because this system provides an ideal model for distinguishing bottom-up and top-down influences, we investigated the processing of visual stimuli and bottom-up and top-down effects in both hemispheres in pigeons. We recorded from single units in the pigeon's left or right nucleus rotundus (Rt), while the ipsilateral and/or contralateral eye were visually stimulated.

In birds, visual information is processed by the thalamofugal and the tectofugal pathway (Fig. 1), which are equivalent to the mammalian geniculocortical and extrageniculocortical visual systems, respectively (Shimizu and Karten, 1993). As a result of the virtually complete decussation of the bird's optic nerves and the limited number of recrossings, both pathways project mainly to the contralateral hemisphere. Whereas behavioral (Deng and Rogers, 2002) and anatomical studies (Koshiba et al., 2003) show the thalamofugal system of chicks to be asymmetrically organized, in pigeons the tectofugal system displays left-right differences (Güntürkün, 2002). The tectofugal pathway consists of retinal projections to the contralateral optic tectum (OT), from which fibers lead bilaterally to Rt, which exclusively projects to the ipsilateral forebrain entopallium (Engelage and Bischof, 1993; Reiner et al., 2004). The crossed component of the tectorotundal system is asymmetrically organized, with more fibers traversing from the right tectum to the left Rt than from the left tectum to the right Rt (Güntürkün et al., 1998). Consequently, a larger number of left rotundal units should integrate binocular input. This kind of asymmetry would exemplify a bottom-up lateralization. However, descending telencephalic pathways also reach the tectum and activate tectal cells (Britto, 1978; Leresche et al., 1983; Dubbeldam et al., 1997). These descending fibers could initiate a second wave of rotundal activation that results from a

Received June 23, 2004; revised Sept. 10, 2004; accepted Sept. 10, 2004.

This work was supported by the Deutsche Forschungsgemeinschaft (Sonderforschungsbereich 509; Neurovision). The original research reported here was performed under guidelines established by the German Welfare Law and was permitted by the responsible state authority. We thank Ariane Schwarz for excellent support and Daniela Schoofs and Martina Manns for helpful comments on this manuscript.

Correspondence should be addressed to Kristian Folta at the above address. E-mail: kristian.folta@ruhr-uni-bochum.de.

DOI:10.1523/JNEUROSCI.3289-04.2004

 0270-6474/04/249475-11$15.00/0

telencephalotectorotundal system. Asymmetries of this latter component would be indicative of top-down left-right differences.

Using a standardized stimulation paradigm, we were able to distinguish different contributions of ascending and descending systems to visual asymmetry within the tectofugal system of the pigeon. This analysis shows that bottom-up signals display gradual left-right differences, whereas top-down influences are organized in a dichotomous all-or-none manner. Such a pattern suggests a cerebral organization in which both hemispheres display some complementary left-right differences in processing various stimulus properties within ascending systems, although the subsequent executive control for these tasks is primarily controlled by the functionally dominant side.

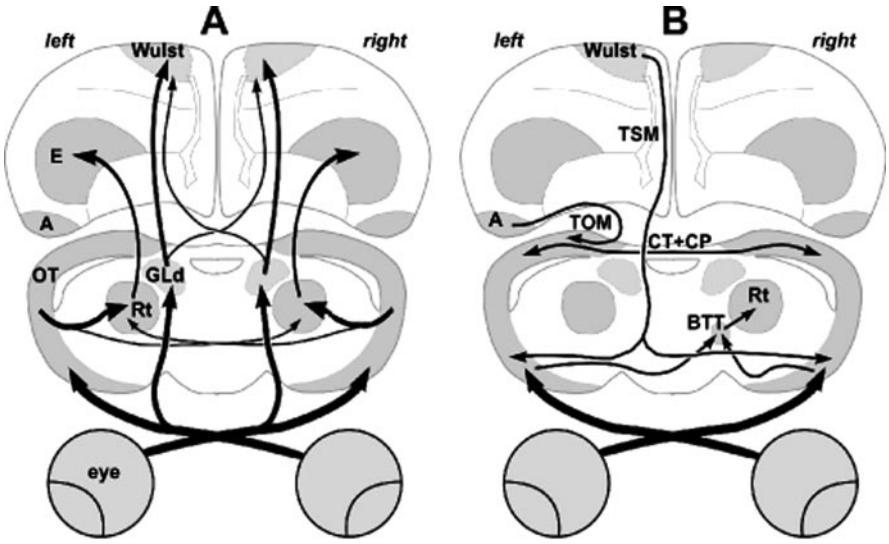

Figure 1. Schematic of the ascending tectofugal and thalamofugal visual pathways (*A*) as well as the descending telencephalotectal and commissural systems (*B*) that affect tectofugal processing in pigeons. The frontal sections that are used do not represent real anatomical crossections but show structures that are normally not visible within a single plain. To avoid confusion, descending telencephalotectal tracts as well as the indirect tectorotundal projection over the bed nuclei of the tectothalamic tract were only drawn for one hemisphere. A, Arcopallium; BTT, bed nuclei of the tectothalamic tract; CT, commissura tectalis; CP, commissura posterior; E, entopallium; GLd, n. geniculatus lateralis, pars dorsalis.

Materials and Methods

Animals. The original research reported herein was performed according to the principles regarding the care and use of animals adopted by the American Physiological Society, the Society for Neuroscience, and the specifications of the German Animal Welfare Law for the prevention of cruelty to animals. A total of 30 adult naive homing pigeons (*Columba livia*) of local origin and both sexes were used for this study.

Surgery and extracellular recording. Before surgery and throughout the recordings, each pigeon was anesthetized by an intramuscular injection of 25% urethane (1 ml/100 gm body weight) and was mounted in a stereotaxic headholder. Stereotaxic coordinates for the electrode positions were derived from the atlas of the pigeon brain (Karten and Hodos, 1967). Body temperature was maintained using an electrical heating pad. The brain was exposed at the appropriate stereotaxic coordinates, and an incision was made in the dura mater. The surface of the brain was covered with mineral oil to prevent it from drying. Finally, the upper and lower eyelids were held open with sticky tape.

Extracellular single-cell responses were recorded in the left Rt from 10 pigeons and in the right Rt from 16 pigeons using glass-coated platinum-iridium electrodes with ~1.0 MΩ resistance. Spikes were amplified and filtered using conventional techniques. Single-unit spikes with a high signal-to-noise ratio (3:1) were sampled at 9600 Hz and were isolated with the aid of the window discriminator of the acquisition program Experimenter's Workbench (DataWave Technologies, Longmont, CO). The spike-sorting and cluster-cutting routine performed off-line allowed us to sort neuronal responses according to shape and amplitude.

At the end of each experimental session, we marked the position of the last electrode and the innermost and outermost borders of all recording sites by inserting a metal electrode and applying a small electrical current for a "Prussian blue" reaction (Green, 1958; Fung et al., 1998). Afterward, all pigeons were perfused intracardially with 100 ml of 0.9% (w/v) sodium chloride followed by 800 ml of ice-cold 4% paraformaldehyde plus 15% potassium ferricyanide (for the Prussian blue reaction) in 0.12 M phosphate buffer, pH 7.4. After the perfusion, the brains were removed from the skull and were postfixed overnight in a 4% solution of paraformaldehyde plus 30% sucrose and 15% potassium ferricyanide. Next, they were cryoprotected for 24 hr with 30% sucrose in 0.12 M phosphate buffer. The brains were sectioned in the saggital plane at 50 μm on a freezing microtome, and the slices were mounted and counterstained with cresyl violet. The sections served for verification of the electrode tracks, which were reconstructed according to the Karten and Hodos (1967) atlas of the pigeon brain.

Visual stimulus presentation. Our stimulation technique should activate most rotundal units in a standardized manner and should enable a discrimination between bottom-up and top-down influences. We therefore used light flashes to activate the ipsilateral and/or the contralateral eye to the recorded hemisphere. Although many rotundal cells respond to moving stimuli (Wang et al., 1993; Sun and Frost, 1998), a substantial proportion is tuned to other aspects, such as color and luminance, without responding to movement (Granda and Yazulla, 1971; Wang et al., 1993). However, because virtually all rotundal units are excited by light flashes (Revzin, 1970; Granda and Yazulla, 1971), this stimulus gave us the maximal probability to obtain recordings from the majority of rotundal units. It also allowed us to rigidly compare response latencies, response durations, and the response strength of cells in both hemispheres after ipsilateral and contralateral stimulation. The Rt was chosen as the target area, because the lateralized organization of recrossing tectorotundal fibers predicted an asymmetry in the bottom-up system (Güntürkün et al., 1998).

Ipsilateral, contralateral, and bilateral light flashes of 500 msec duration (the terms refer to the position of the recording electrode in Rt) were produced by a 15 V, 150 W halogen light with a luminance of 40 cd/m^2. The light was gated by two mechanical shutters and was transmitted to the bird's eyes by two oculars of 15 cm length and with a diameter of 1.5 cm. They were arranged in an angle of ~60° to the left and right from midline, corresponding to the optical axis. This guaranteed that light was transferred only to the appropriate eye. The background illumination was 5 lux.

The data acquisition started 100 msec before stimulus onset, which was defined as the point in time when luminance had reached 10% of its maximum. Each unit was stimulated with ipsilateral, contralateral, and bilateral light flashes. A control condition without stimulation was used for the measurement of spontaneous cell activity. Under each of these conditions, spike trains of 1 sec duration were acquired over 10–50 trials (dependent on the quality and stability of cell responses). The interstimulus time was 5 sec.

Data analysis. Spike activity was measured during ipsilateral, contralateral, and bilateral stimulation conditions within the first 250 msec time interval after stimulus onset. Dependent *t* test comparisons confirmed the statistical significance ($p < 0.05$) of all cell responses from spontaneous cell activity. Peristimulus-time histograms (PSTHs) with binwidths of 5 msec were calculated over all repetitions of each stimulation condition. The number of repetitions was taken into account by

dividing the absolute number of spikes per sec (for each 5 msec bin) by the total number of repetitions recorded for each neuron.

For the analyses of response latencies, response durations, and response strengths, normalized PSTHs were calculated by dividing the number of spikes for each 5 msec bin by the maximum number of spikes per bin for each stimulation condition, resulting in bin values between 0 and 1. After that, we calculated the first 5 msec bin of each neuron and stimulation condition for which the normalized cell response was 20% above zero. The lower time limit of this bin was taken as an estimate of response latency if this bin was immediately followed by a second bin above threshold. Additionally, we calculated the upper time limit of the last bin that was followed by at least two bins under threshold. These calculations were done for every response component of each stimulation condition. The difference of the lower and upper time limit of each response component was taken as an estimate of response duration. According to the calculated values of response latency and response duration, we defined an interval for which the mean response strength was calculated. Finally, dependent *t* tests and ANOVAs were used to test for differences in response latency, duration, and strength of early and late response components in the left and right hemisphere.

For the analyses of the effects of Wulst inactivation on the response characteristic of rotundal cells, we calculated the mean of activity before and 20 min after injections of lidocaine in every 5 msec bin for each cell and stimulation condition. We normalized these data by dividing the number of spikes for each 5 msec bin by the maximum number of spikes per bin that we obtained in all stimulation conditions of one cell. This resulted in normalized PSTHs with spike values between 1 and 0. We averaged the individual cell responses by calculating the mean activity for each 5 msec bin and then calculated the difference of the mean of normed spike values in the lidocaine and the pretest and post-test conditions for each stimulation condition. From these data, histograms were created with positive values indicating excitatory influences and negative values inhibitory influences onto rotundal units after the blocking of visual Wulst efferents. According to these histograms and the calculated values of response latency and response duration, we defined intervals for which the mean response strengths were calculated. Finally, ANOVAs were used to test for selective effects of lidocaine injections on the response characteristics of rotundal cells.

Classification of cells. All cells were classified according to their response characteristics. Cells with response latencies of <60 msec after stimulus onset were classified as bottom-up processing types, referring to the ascending tectofugal processing from the retina via the contralateral OT to the ipsilateral Rt. The maximal time limit of 60 msec was chosen on the basis of previous studies that demonstrate that tectal latencies start at a minimum of 25.6 msec (Letelier et al., 2000). Given the necessary delay for the ignition of tectal relay cells and the subsequent conduction time to the ipsilateral Rt, thalamic latencies between 30 and 40 msec were expected (Webster, 1974; Letelier et al., 2000). This correlates well with the data of Schmidt and Bischof (2001), who reported latencies of 30.7 msec after contralateral photic eye stimulation in the zebra finch. Cells exclusively showing response components with latencies of longer than 70 msec were classified as top-down processing types, indicating the involvement of processing pathways that feed back from forebrain structures via the OT to the Rt. The minimal limit of 70 msec was chosen on the basis of studies demonstrating that electrical Wulst stimulation must precede optic nerve stimulation by 30–100 msec to be effective on single tectal neurons (Bagnoli et al., 1977; Britto, 1978). Because electrical stimulation produces considerably shorter latencies within the tectofugal system (Bagnoli et al., 1982; Letelier et al., 2000), top-down signals most likely need longer than 70 msec to arrive at rotundal level. By defining nonoverlapping latency criteria of shorter than 60 msec for bottom-up and longer than 70 msec for top-down responses, we aimed to distinguish these two sources of afferents. Cells containing response components of both short (<60 msec) and long (>70 msec) response latency were classified as mixed processing neurons, assuming they contain response components transferred by both tectorotundal and forebrain mediated pathways. These arguments are outlined in detail in the discussion of this article.

Visual Wulst inactivation of top-down response components. In four pigeons, we investigated the origin of top-down response components through reversible lidocaine inactivations of the visual Wulst. Based on stereotaxic coordinates, bone, and dura overlying, the Wulst were removed. Lidocaine injections were performed by means of a glass pipette (~25 μm tip diameter) connected to a 50 μl Hamilton syringe that was filled with 4% lidocaine (Sigma, St. Louis, MO) in 0.12 M PBS, pH 7.4. The tip of the pipette was positioned stereotaxically (Karten and Hodos, 1967) into the left hyperpallium apicale (HA) of the Wulst. After placing a recording electrode into the left Rt (see *Surgery and extracellular recording*) and identifying a mixed processing cell type with response components of short and long latency, we started to record cell responses to light stimulation of the contralateral and/or the ipsilateral eye (see *Visual stimulus presentation*). Then, 1 μl of lidocaine was injected into HA before the responses to ipsilateral, contralateral, and bilateral light flashes were tested for a second time. HA is the origin of the tractus septomesencephalicus (TSM) that descends to various subtelencephalic structures, including the tectum. The lidocaine injection therefore caused a temporal inactivation of Wulst efferents to the OT. The effective spread of 1 μl of lidocaine has been investigated by Sandkühler et al. (1987) and Martin (1991) and was estimated to have a radius of 1.4–1.7 mm. Because the HA of the pigeon Wulst extends 14.5–7.5 mm anterior of interaural zero and is up to 3–4 mm in the medial-lateral dimension (Karten and Hodos, 1967), we were confident that our lidocaine injection temporarily inactivated a major portion of the afferents from the Wulst onto the tectum. We confirmed the reversibility of the lidocaine effects by recording from the same neuron a final time after a 20 min wash-out period.

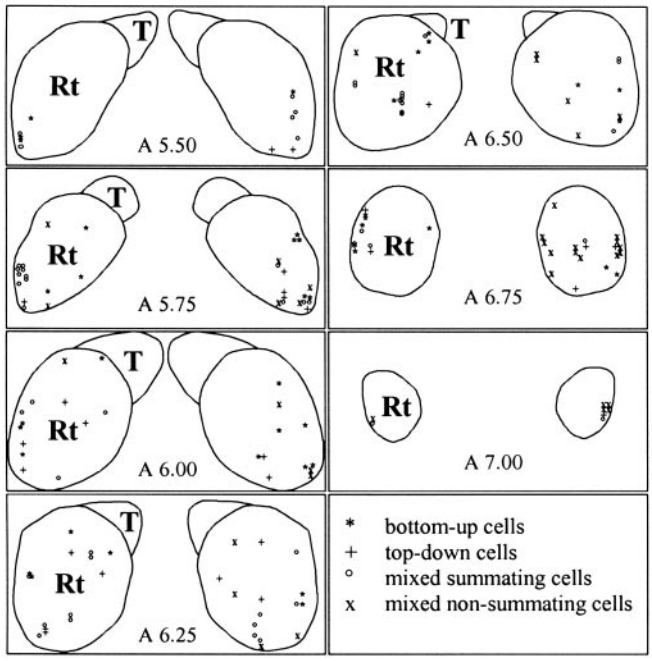

Figure 2. Distribution of electrophysiological recording sites histologically identified in the left and the right Rt. Anteroposterior levels (A) are according to the atlas by Karten and Hodos (1967). T, Nucleus triangularis.

Results

Identification of recording positions

We successfully isolated 76 neurons from the left and 86 neurons from the right Rt. Four additional rotundal cells of the mixed type were isolated in the left hemisphere for studying selective effects of lidocaine onto early and late rotundal response components. The location of Prussian blue marks and the reconstruction of the electrode tracks confirmed that all recorded cells were within Rt. Our recordings were made from virtually all areas of the nucleus. No regional clustering of different cell types was visible (Fig. 2).

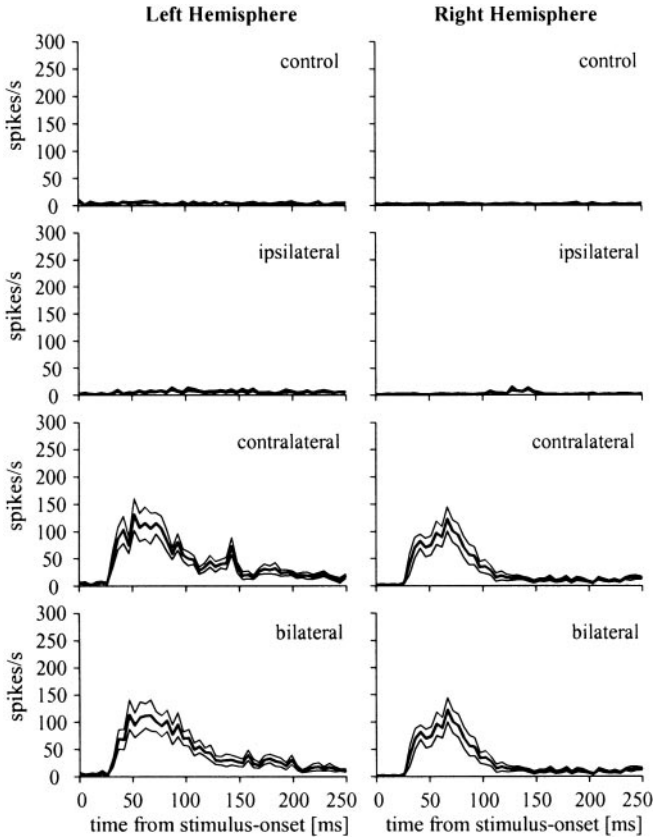

Figure 3. Averaged responses of rotundal bottom-up cell types in the control condition and after ipsilateral, contralateral, and bilateral eye stimulation. Data are shown for the left and the right hemisphere. Solid thick lines represent the mean of spike activity and thin lines the SE for all bins. Bin width is 5 msec.

General analysis of rotundal cell responses

Most rotundal responses consisted of a burst of spikes to the onset of the light flash. All neurons were spontaneously active with an average firing rate of 3.2 spikes/sec. Visual stimulation of the ipsilateral eye led to a noticeable increase in firing rate to an average of 11.2 spikes/sec. Stimulation of the contralateral eye led to a mean firing rate of 32.2 spikes/sec, and bilateral stimulation produced mean firing rates of 39.6 spikes/sec. A two × four ANOVA with hemisphere (left and right) as between-subjects factor and the stimulation condition (control, contralateral, ipsilateral, and bilateral stimulation) as repeated-measures factor revealed no significant differences between the activity of neurons in the left and the right Rt ($F_{(1,160)} = 0.029$; $p < 0.864$) but a significant main effect of stimulation condition ($F_{(3,480)} = 273.87$; $p < 0.001$). *Post hoc* comparisons with Scheffé tests revealed that ipsilateral stimuli generally elicited significantly lower average spike rates than contralateral and bilateral stimuli ($p < 0.001$) but were significantly different from spontaneous activity ($p < 0.001$). Additionally, the ANOVA revealed a significant two-way interaction of the factors hemisphere and stimulation condition ($F_{(3,480)} = 7.839$; $p < 0.001$). This interaction was attributable to qualitative differences in the response characteristics of long latency response components (top-down responses) that were exclusively triggered by the right-eye system. We will refer to this point later on in this section.

Analysis of bottom-up processing cells

Figure 3 shows the averaged responses of rotundal bottom-up cells for the different stimulation conditions in the left and the right hemisphere. Analysis of cell responses revealed short latency response components exclusively after contralateral and bilateral stimulation of the eyes. After contralateral stimulation, we observed a mean response latency of 45.5 msec, response duration of 77.5 msec, and response strength of 108.4 spikes/sec for the left Rt. For the right Rt, we saw a mean latency of 37.9 msec, response duration of 56 msec, and response strength of 103.2 spikes/sec (Fig. 4*A–C*). When stimulated bilaterally, all cells showed nearly identical response characteristics. We observed a binocular mean response latency of 47.3 msec, a response duration of 76.8 msec, and a response strength of 109.4 spikes/sec in the left Rt, compared with a mean latency of 39.5 msec, a duration of 56 msec, and a response strength of 95.9 spikes/sec in the right hemisphere (Fig. 4*A–C*). Therefore, under both stimulation conditions, the response latency was ~8 msec longer and the mean response duration ~21 msec longer in the left than in the right hemisphere. Two × two ANOVAs with hemisphere as the between-subjects factor and stimulus condition (contralateral, bilateral) as the within-subjects factor revealed a significant main effect of the between-subjects factor hemisphere for the analysis of response latencies ($F_{(1,41)} = 4.527$; $p < 0.039$) and response durations ($F_{(1,41)} = 4.079$; $p < 0.049$) but no significant main effect for the analysis of response strengths ($F_{(1,41)} = 0.302$; $p < 0.586$). Furthermore, we obtained significant differences between contralateral and bilateral stimulations in the response latency ($F_{(1,41)} = 10.831$; $p < 0.002$) but no significant effect of stimulus condition on response durations ($F_{(1,41)} = 0.013$; $p < 0.912$) and response strengths ($F_{(1,41)} = 1.049$; $p < 0.312$). There was no significant interaction between the factors stimulus condition and hemisphere ($p > 0.05$).

Analysis of top-down processing cells

Figure 5 shows the averaged responses of top-down cells in the left and the right hemisphere for the different stimulation conditions. Whereas bottom-up processing cells showed exclusively short latency response components after monocular and binocular stimulation, top-down processing cells were characterized by response components with an extremely long response latency. We observed a mean latency of 120 msec, a short response duration of 27.5 msec, and a response strength of 113.2 spikes/sec in the left Rt and in the right Rt, a mean latency of 126.7 msec, a response duration of 24 msec, and a response strength of 143.6 spikes/sec (Fig. 6*A–C*). In the left Rt, we observed these monocular response components exclusively after contralateral stimulation of the right eye and in the right Rt, only after ipsilateral stimulation of the right eye. This "triggering" effect of the right-eye system is able to explain the significant two-way interaction of the factors hemisphere and stimulation condition that we mentioned at the beginning of this section (see *General analysis of rotundal cell responses*).

When top-down classified cells were stimulated binocularly, they showed reduced long latency components (compared with the long latency components in the monocular stimulation conditions) with a mean response latency of 74.2 msec and a response duration of 86.7 msec in the left Rt and a mean latency of 80.3 msec and a response duration of 83.7 msec in the right Rt. The mean response strength decreased to 59.7 spikes/sec in the left Rt and to 92.2 spikes/sec in the right Rt. Two × two ANOVAs with hemisphere as between-subjects factor and response components (late binocular vs late monocular components) as within-subjects factor revealed the reduction of response latency

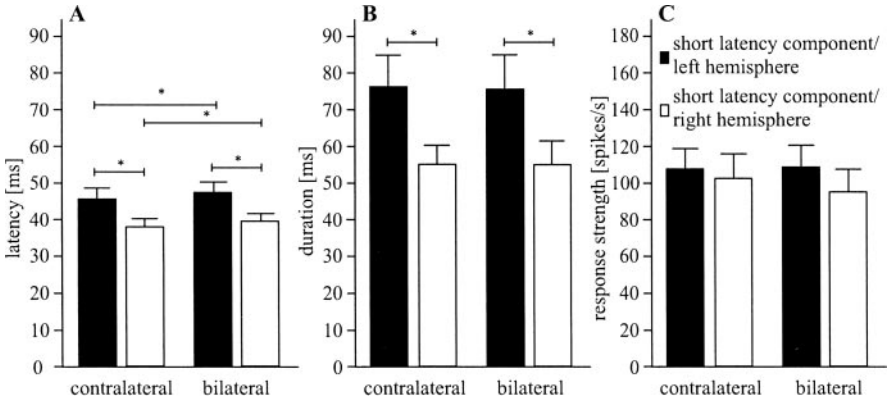

Figure 4. Mean response latencies (*A*), response durations (*B*), and response strengths (*C*) of bottom-up cell types in the left (black) and the right (white) hemisphere after contralateral and bilateral eye stimulation. Error bars depict SE. Asterisks indicate significant differences at the 5% level.

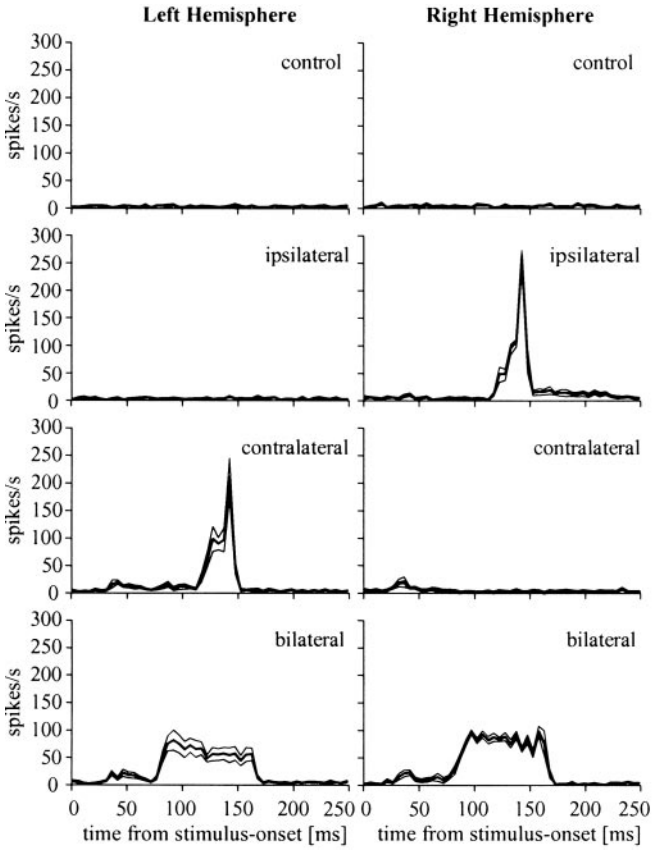

Figure 5. Averaged responses of rotundal top-down cell types in the control condition and after ipsilateral, contralateral, and bilateral eye stimulation. Data are shown for the left and the right hemisphere. Solid thick lines represent the mean of spike activity and thin lines the SE for all bins. Bin width is 5 msec.

($F_{(1,25)} = 279.523$; $p < 0.001$), the enhancement of response duration ($F_{(1,25)} = 242.26$; $p < 0.001$), and the reduction of response strength ($F_{(1,25)} = 34.574$; $p < 0.001$) to be highly significant. There were significant hemispheric differences of response latencies ($F_{(1,25)} = 6.644$; $p < 0.016$) but no significant differences of response durations ($F_{(1,25)} = 0.709$; $p < 0.408$) and response strengths ($F_{(1,25)} = 4.239$; $p < 0.0501$) and no significant interactions of response components and hemisphere ($p > 0.05$).

Analysis of mixed nonsummating cells

Mixed processing neurons showed components of both short and long response latency. We classified all mixed processing neurons into two subtypes based on their integration of short and long latency information after simultaneous light stimulation of both eyes. Mixed nonsummating cells always ignored long latency information in their bilateral cell responses, whereas mixed summating cells exhibited a nonlinear integration of early and late response components after stimulating both eyes.

Figure 7 shows the averaged responses of mixed nonsummating cells in the left and the right hemisphere for the different stimulation conditions. After stimulation of the contralateral eye, cells in the left Rt had a response component with a short mean response latency of 32 msec, a response duration of 49 msec, and a mean response strength of 221.5 spikes/sec; cells in the right Rt had a mean latency of 33.9 msec, a duration of 67.6 msec, and a response strength of 133.5 spikes/sec. These responses were almost identical to the short latency components after binocular stimulation with a mean latency of 35 msec, a response duration of 67 msec, and a response strength of 200.8 spikes/sec in the left Rt and a latency of 35.3 msec, a duration of 63.6 msec, and a response strength of 139 spikes/sec in the right Rt (Fig. 6*A–C*).

Furthermore, all mixed nonsummating cells in the left Rt, but no cells in the right Rt, showed an additional short latency response component after stimulation of the ipsilateral eye. The mean response latency of 52 msec after ipsilateral eye stimulation was ~17–20 msec longer than short latency components after contralateral and bilateral eye stimulation. Dependent *t* tests revealed significant differences between early ipsilateral and early contralateral ($t_{(4)} = 4.216$; $p < 0.014$) or bilateral response latencies ($t_{(4)} = 4.543$; $p < 0.011$) but no significant differences of response duration (dependent *t* test; $p > 0.05$). Response strength was found to be significantly less for the short latency response after ipsilateral stimulation (83 spikes/sec) than for the early response components after contralateral ($t_{(4)} = 4.536$; $p < 0.011$) or binocular stimulation ($t_{(4)} = 6.011$; $p < 0.004$).

In addition to the short latency response components, mixed nonsummating cell types in both hemispheres exhibited long latency response components after monocular light stimulation with a mean latency of 125 msec, a response duration of 21 msec, and a response strength of 147.1 spikes/sec in the left Rt and a mean latency of 113.7 msec, a duration of 45.3 msec, and a response strength of 63.6 spikes/sec in the right Rt (Fig. 6*A–C*). As in top-down processing cells, these long latency response components were triggered exclusively by the right-eye system. They could therefore be observed in the left Rt exclusively after contralateral and in the right Rt only after ipsilateral stimulation of the right eye.

We analyzed the latencies, durations, and strengths of cell responses (with exception of early ipsilateral responses) with two × three ANOVAs with hemisphere as the between-subjects factor and response components (early monocular, early binocular, and late monocular components) as the within-subjects factor. These analyses revealed significant main effects for the factor response components for the comparisons of response latencies ($F_{(2,68)} = 420.799$; $p < 0.001$), response durations ($F_{(2,68)} =$

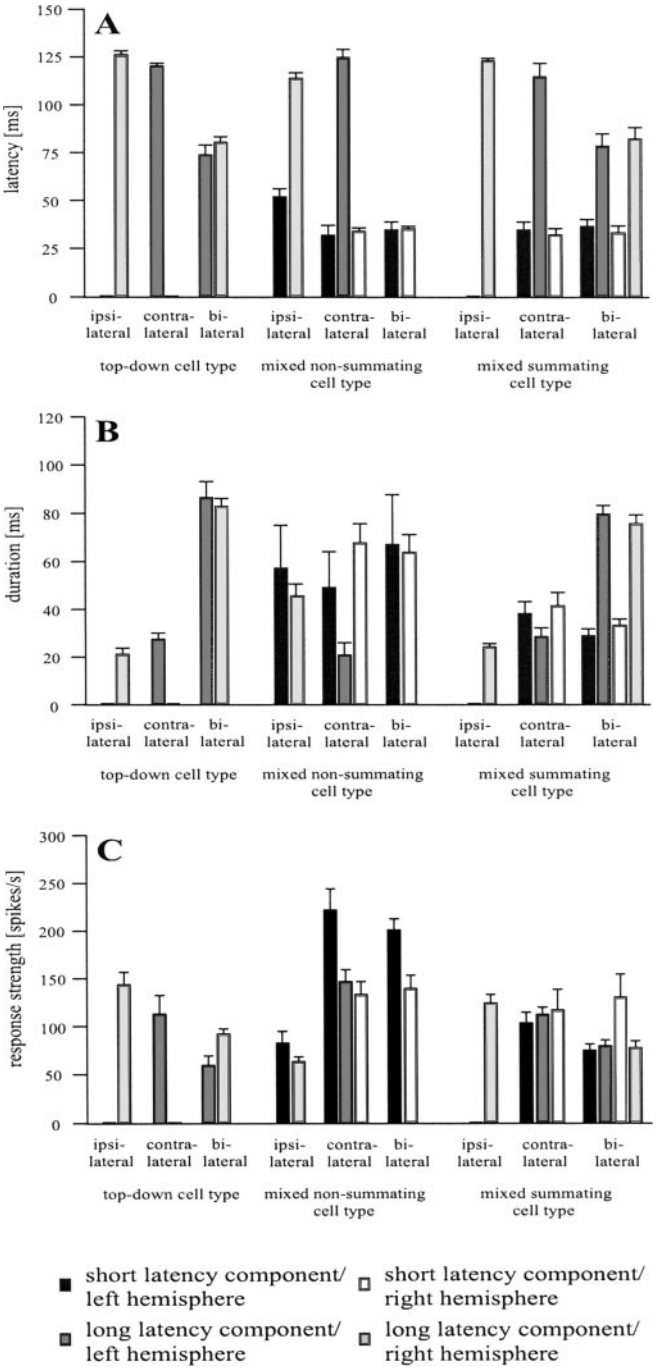

Figure 6. Mean response latencies (*A*), response durations (*B*), and response strengths (*C*) of top-down, mixed nonsummating, and mixed summating cell types in the left and the right hemisphere after ipsilateral, contralateral, and bilateral eye stimulation. Error bars depict SE. To avoid confusion, significant differences are not depicted on top of the bars but are reported in Results.

6.562; $p < 0.003$), and response strengths ($F_{(2,68)} = 12.917$; $p < 0.001$). *Post hoc* comparisons with Scheffé tests confirmed that long latency components differed significantly from short latency components ($p < 0.001$), but there were no significant differences between early contralateral and bilateral response components ($p > 0.05$). Only the analysis of response strength revealed a significant main effect of the factor hemisphere ($F_{(1,34)} = 10.857$; $p < 0.002$). The mean response strength in the left hemisphere was significantly higher than in the right hemisphere.

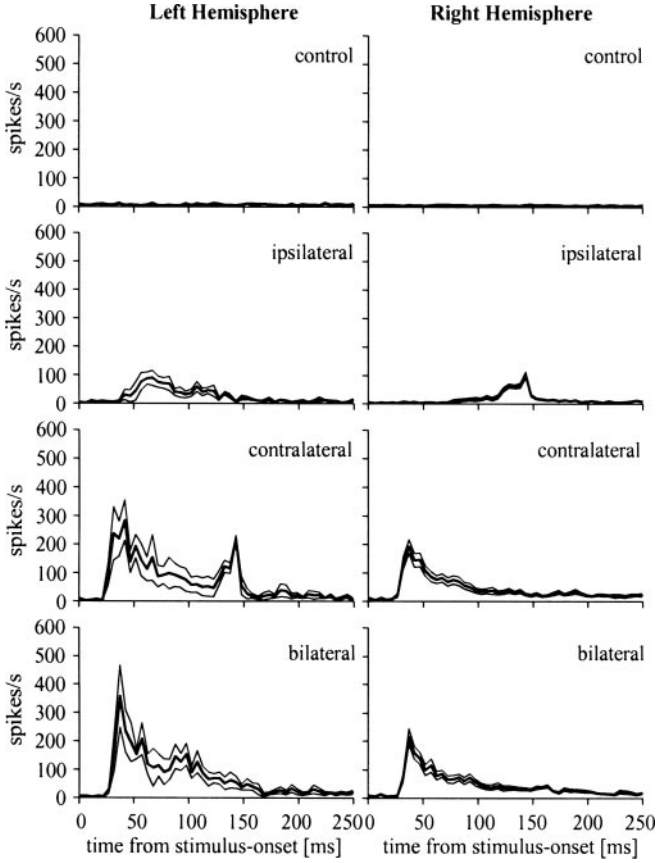

Figure 7. Averaged responses of rotundal mixed nonsummating cell types in the control condition and after ipsilateral, contralateral, and bilateral eye stimulation. Data are shown for the left and the right hemisphere. Solid thick lines represent the mean of spike activity and thin lines the SE for all bins. Bin width is 5 msec.

There were no significant interactions between the factors hemisphere and response components.

Analysis of mixed summating cells

Mixed summating cells differed from mixed nonsummating cells in their response characteristic after binocular visual stimulation. Figure 8 shows the averaged responses of this cell type in the left and the right hemisphere for the different stimulation conditions. After stimulation of the contralateral eye, these cells responded with a short mean latency of 38.4 msec, a response duration of 38.1 msec, and a response strength of 103.8 spikes/sec in the left Rt and with a mean latency of 33.7 msec, a duration of 41.3 msec, and a response strength of 117 spikes/sec in the right Rt (Fig. 6*A–C*).

Additionally, we observed long latency components after monocular stimulation with a mean response latency of 117 msec, a response duration of 29.7 msec, and a response strength of 112.5 spikes/sec in the left Rt and with a latency of 123.2 msec, a duration of 24.2 msec, and a response strength of 124.1 spikes/sec in the right Rt (Fig. 6*A–C*). These components were again exclusively triggered by the right-eye system and could therefore be obtained in the left Rt only after contralateral and in the right Rt exclusively after ipsilateral stimulation of the right eye.

When both eyes were stimulated simultaneously, mixed summating cells showed two response peaks. In the left Rt, a short latency response component with a mean latency of 38.7 msec, a duration of 28.8 msec, and a response strength of 75.2 spikes/sec was followed by a second response component with a mean la-

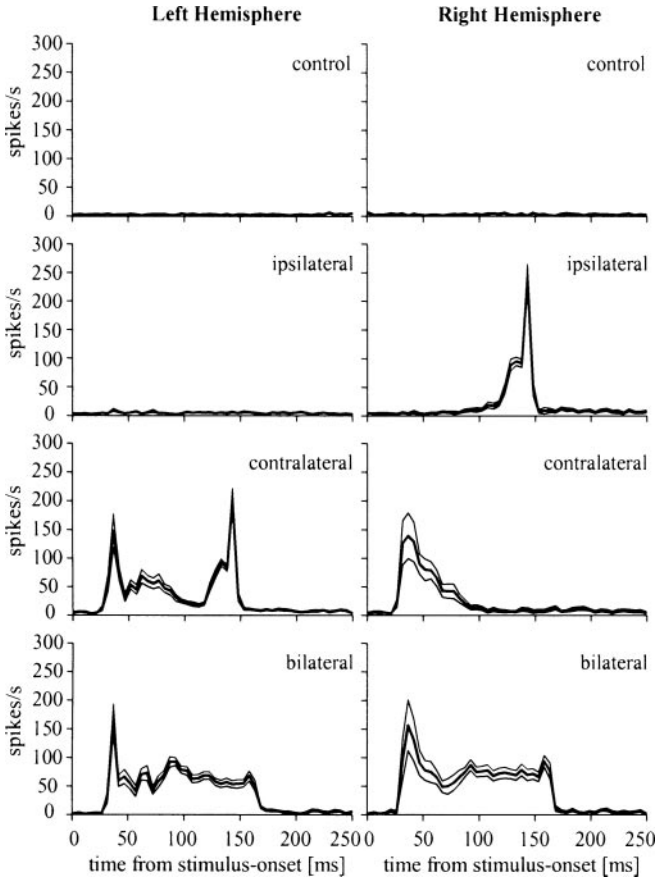

Figure 8. Averaged responses of rotundal mixed summating cell types in the control condition and after ipsilateral, contralateral, and bilateral eye stimulation. Data are shown for the left and the right hemisphere. Solid thick lines represent the mean of spike activity and thin lines the SE for all bins. Bin width is 5 msec.

tency of 81.1 msec, a duration of 80 msec, and a response strength of 79.9 spikes/sec. This was comparable with the right Rt with a first peak with a mean latency of 35.3 msec, a response duration of 33.4 msec, and a response strength of 130.6 spikes/sec that was followed by a second response component with a mean response latency of 85.3 msec, a duration of 75.8 msec, and a response strength of 77.3 spikes/sec (Fig. 6*A–C*). This binocular response characteristic revealed a nonlinear summation of early and late monocular response components. As in top-down classified cells, the late binocular response components showed a reduction in response latency from ~120 msec after monocular to ~83 msec after binocular stimulation and an elongated response duration from ~27 to ~78 msec (Fig. 6*A–C*).

Two × four ANOVAs with the factors hemisphere and response components (early monocular, early binocular, late monocular, late binocular components) revealed a significant main effect of the factor response components for the statistical comparisons of response latency ($F_{(3,162)} = 659.756$; $p < 0.001$), response duration ($F_{(3,162)} = 69.004$; $p < 0.001$), and response strength ($F_{(3,162)} = 8.383$; $p < 0.001$). *Post hoc* comparisons with Scheffé tests revealed significant differences in response latency ($p < 0.001$) and response duration ($p < 0.05$) between short and long latency components after monocular stimulation and a significant reduction of response latency, a significant enhancement of response duration, and a significant reduction of response strength of monocular long latency components after binocular eye stimulation ($p < 0.001$). There were no significant differences between early contralateral and bilateral response components and no significant main effect of the factor hemisphere ($p > 0.05$).

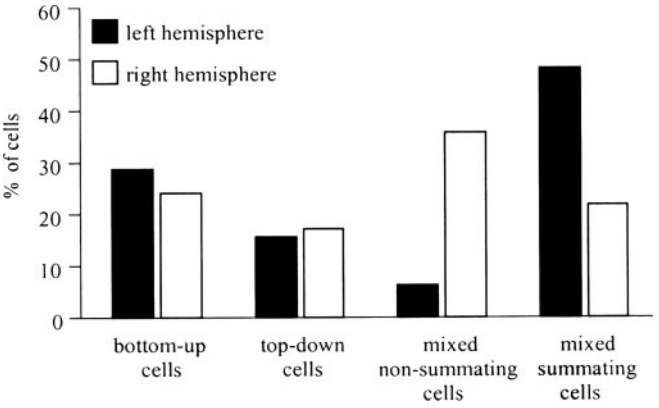

Figure 9. Distribution of different cell types in the nucleus rotundus of both hemispheres.

Distribution of cells in the left and the right hemisphere

As shown in Figure 9, 28.95% of all recorded cells in the left and 24.42% of cells in the right Rt were classified as bottom-up processing cell types. Only 15.79% of cells in the left and 17.44% of cells in the right Rt were classified as top-down types. These data indicate an equal distribution of these cell types in the left and the right hemisphere, in contrast to mixed summating and mixed nonsummating cells that showed an asymmetric distribution in the left and the right brain (Fig. 9). Mixed nonsummating cells that exhibited both early and late response components, but ignored the late component when both eyes were stimulated simultaneously, comprised a portion of 6.58% in the left and 36.05% in the right Rt. Alternatively, mixed summating cells that showed a nonlinear integration of early and late response components after binocular eye stimulation made up 48.68% of cells in the left Rt and only 22.09% of cells in the right Rt. This integration produced a spiking interval ~45 msec longer than mixed nonsummating cells that lost the long latency component in bilateral responses. This asymmetry indicates that most mixed processing cells in the left Rt respond significantly longer to binocular visual input than do cells in the right hemisphere.

Effects of Wulst inactivation

To make sure that our classification of early and late components as tectally or as forebrain derived is probably correct, we isolated four left rotundal mixed summating cell types (see *Analysis of mixed summating cells*) in four pigeons and injected lidocaine into the left visual Wulst. Figure 10 shows the effects of Wulst inactivation onto rotundal cells in each stimulation condition (control, ipsilateral, contralateral, and bilateral presented stimuli). Additionally, the differences between normalized spike values obtained immediately after the lidocaine injection and the mean of spike values obtained before and 20 min after the injection are depicted (Fig. 11). Positive and negative values indicate excitatory and inhibitory effects of Wulst blockade onto rotundal responses, respectively. As depicted, lidocaine injections were followed by irregular spike frequency changes of early rotundal responses and a systematic inhibitory effect of middle and late responses. Three × four ANOVAs on the non-normalized response strengths data with the repeated-measures factors injection condition (pretest, lidocaine injection, post-test) and stimulation condition (control, contralateral, ipsilateral, bilateral)

were used to test for significant effects of the blocking of Wulst efferents by lidocaine on the rotundal response strength. We separately analyzed the changes in activity 30–70 msec, 80–160 msec, and 115–140 msec after stimulus presentation to control for changes in all relevant periods.

The analysis of lidocaine effects on the responses 30–70 msec after stimulus onset revealed a significant main effect of the factor stimulation condition ($F_{(3,9)} = 43.143$; $p < 0.001$) but no significant main effect of the factor injection condition ($F_{(2,6)} = 0.417$; $p < 0.677$) and no significant interaction ($F_{(6,18)} = 0.391$; $p < 0.875$). *Post hoc* comparisons with Scheffé tests showed significant differences ($p < 0.001$) of activity in the control condition (2.7 spikes/sec) and after ipsilateral stimulation (6.9 spikes/sec) compared with spike activity after contralateral (82.8 spikes/sec) and bilateral stimulation (85 spikes/sec). There were no significant differences of activity in the control condition compared with activity after ipsilateral stimulation ($p = 0.979$) and no differences of activity after contralateral and bilateral eye stimulation ($p = 0.997$).

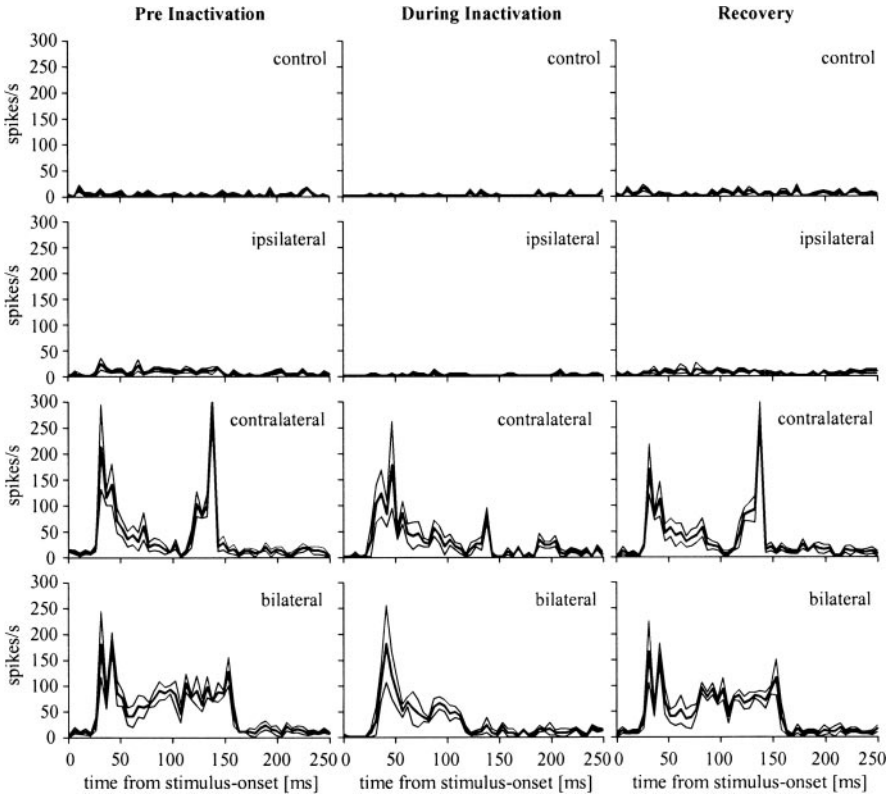

Figure 10. Averaged responses of left rotundal mixed summating cell types under different stimulation conditions before, during, and after inactivation of the left Wulst. Solid thick lines represent the mean of spike activity and thin lines the SE for all bins. Bin width is 5 msec.

The analysis of responses 80–160 msec after stimulus onset revealed a significant effect of the main factors injection condition ($F_{(2,6)} = 16.501$; $p < 0.004$) and stimulation condition ($F_{(3,9)} = 59.388$; $p < 0.001$) and a significant interaction of both factors ($F_{(6,18)} = 11.067$; $p < 0.001$). *Post hoc* comparisons with Scheffé tests showed that the mean response strengths of 36 spikes/sec before and of 34.6 spikes/sec 20 min after the Wulst injection became significantly reduced to a response strength of 13.5 spikes/sec directly after lidocaine application ($p < 0.01$). There were no significant differences between the response strengths in pretests and post-tests ($p = 0.95$). The *post hoc* analysis of the effects of the different stimulation conditions revealed a significant enhancement of spike activity after contralateral and bilateral stimulation compared with the activity in the control condition or after ipsilateral stimulation ($p < 0.001$). Furthermore, the activity resulting from contralateral stimulation (41.1 spikes/sec) was significantly lower ($p < 0.05$) than the activity obtained after bilateral stimulation (62.2 spikes/sec), but there was no significant difference ($p = 0.965$) between the activity after ipsilateral stimulation (5.7 spikes/sec) and the control condition (3 spikes/sec). The significant interaction of the main factors was attributable to these small differences in activity in the ipsilateral and control condition and can therefore be disregarded.

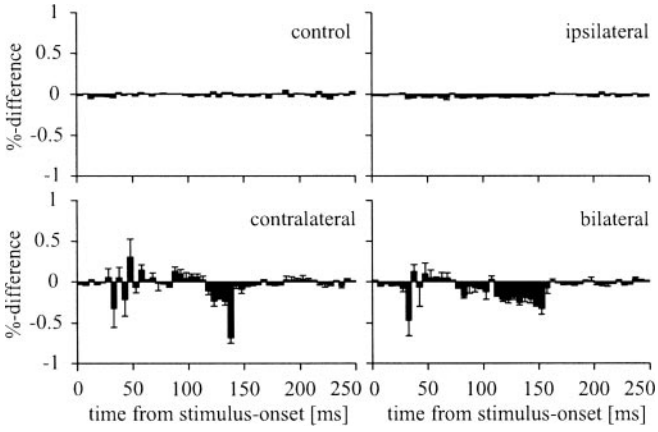

Figure 11. Effects of Wulst inactivation on neuronal response patterns under different stimulation conditions. The time histograms show changes of spike activity, with positive values indicating an excitatory and negative values indicating an inhibitory influence of Wulst blockade onto rotundal neurons. Error bars depict SE. Bin width is 5 msec.

Responses obtained 115–140 msec after stimulus onset showed significant effects of the main factors injection condition ($F_{(2,6)} = 47.592$; $p < 0.001$) and stimulation condition ($F_{(3,9)} = 62.944$; $p < 0.001$) and a significant interaction of both factors ($F_{(6,18)} = 35.163$; $p < 0.001$). *Post hoc* comparisons with Scheffé tests showed a significant reduction of response strength in the lidocaine condition (11.4 spikes/sec) compared with the mean activity before (53.5 spikes/sec) and after (51.3 spikes/sec) the injection ($p < 0.001$). There was no significant difference of activity before and after the injection ($p = 0.899$). *Post hoc* analyses of the effects of the different stimulation conditions revealed a significant enhancement of spike activity after contralateral and bilateral stimulation compared with activity in the control condition or after ipsilateral stimulation ($p < 0.001$). Furthermore, activity after contralateral stimulation (89.5 spikes/sec) was significantly higher ($p < 0.01$) than activity observed after bilateral stimulation (55.3 spikes/sec), but there was no significant difference ($p = 0.997$) between the mean activity after ipsilateral stimulation (5.8 spikes/sec) and the control condition (4.2 spikes/sec). Again, the significant interaction of the main factors was

attributable to these small differences in activity in the ipsilateral and control condition and can therefore be disregarded.

To summarize, we obtained a significant reduction of late response components resulting from a temporal blockade of Wulst efferents. This blockade affects late bilateral plateau components between 80–160 msec as well as late contralateral cell responses between 115–140 msec after stimulus onset. This result pattern shows that the Wulst is a relevant structure that exerts influence on Rt and shapes neuronal responses to visual stimuli.

Discussion

The present study provides a detailed analysis of bottom-up and top-down processes at single-cell level in Rt. Different cell types were found with lateralized processing characteristics within the pigeon's ascending and descending visual pathways.

Tectofugal bottom-up pathways

Synaptic transmission in the retinorecipient tectal layers begins 25.6 msec after contralateral photic activation (Letelier et al., 2000). Because retinotectal terminals are composed of the finest unmyelinated axons (Karten et al., 1997), the observed latencies of early response components most likely stem from a direct tectorotundal projection. They also correspond with rotundal response latencies observed in zebra finches (Schmidt and Bischof, 2001). Tectal lamina 13 neurons project not only to the ipsilateral Rt but also through the dorsal supraoptic decussation (DSO) to the contralateral Rt (Bischof and Niemann, 1990; Güntürkün et al., 1993; Mpodozis et al., 1996). Axon lengths of crossing tectorotundal projections exceed those of ipsilaterally projecting fibers by ~9 mm. The average fiber diameter of myelinated axons in the DSO is 1 μm (Saleh and Ehrlich, 1984), and a distance of 9 mm takes ~4.5 msec to traverse (Rushton, 1951). Adding this to the latency of left rotundal bottom-up responses after contralateral eye stimulation yields 50–51.8 msec. This is virtually identical to the latency of 52 msec that we obtained in left rotundal cells after an ipsilateral light flash and to the latency of 50 msec that was obtained under comparable conditions in zebra finches (Schmidt and Bischof, 2001).

Top-down influences onto the tectofugal system

Most rotundal cells showed response components with latencies longer than 120 msec. It is unlikely that these latencies arise from intratectal activity patterns. Possibly, they reflect a top-down influence from the forebrain. The two telencephalotectal pathways are the TSM, originating mainly in the Wulst (Miceli et al., 1987), and the tractus occipitomesencephalicus (TOM), originating in the arcopallium (Zeier and Karten, 1971; Dubbeldam et al., 1997) (Fig. 1*B*). The TSM receives visual information via the thalamofugal pathway (Güntürkün et al., 1993), whereas the arcopallium receives visual input from the entopallium (Husband and Shimizu, 1999) and a small projection from the Wulst (Shimizu et al., 1995). Photic eye stimulations produce responses with latencies of 40 msec in the arcopallium of the chicken (Yano, 1976). Because the latencies of Wulst neurons are in the range of 18.4–20 msec (Perisic et al., 1971; Gusel'nikov et al., 1976), the first visually triggered top-down effects are possibly mediated by TSM and not TOM.

The TSM terminates predominantly within tectal lamina 13 where it connects to rotundal neurons (Miceli et al., 1987). An electrical stimulation of the Wulst has to precede optic nerve stimulation by 30–100 msec to effectively activate tectal units (Bagnoli et al., 1977; Britto, 1978). If these values are added to the latencies of early response components, the resulting time frame is compatible with the observed latencies of late response components after monocular or binocular stimulation. Blocking visual Wulst efferents with lidocaine significantly decreases late response components, whereas early components were not significantly affected. This illustrates that our classification of early and late components as tectally or as forebrain derived is probably correct.

Additionally, we observed a significant latency reduction of top-down components after bilateral eye stimulation. This indicates that a binocular tectal input probably modifies rotundal responses. Furthermore, it provides strong evidence for an interhemispheric interaction after binocular eye stimulation. Two explanations for this are conceivable. The first is a mechanism mediated via the mainly inhibitory intertectal commissures (Robert and Cuénod, 1969; Hardy et al., 1984). The other involves a cluster of GABAergic structures collectively called the bed nuclei of the tectothalamic tract. These nuclei receive a side branch of the tectorotundal projection from both halfbrains (Theiss et al., 2003) and are involved in the regulation of ipsilateral and bilateral visual input in Rt (Voss and Bischof, 2003).

Asymmetries in bottom-up and top-down processing

Bottom-up asymmetries

Left rotundal bottom-up cells displayed longer latencies to contralateral and bilateral stimulation, and the duration of neuronal activity levels lasted longer on the left side. Additionally, some left-rotundal units represented responses delivered to the ipsilateral eye, whereas this kind of integration was absent on the right side.

The faster right-rotundal responses might enable the right tectofugal system to guide fast visuomotor responses to visual stimuli. Indeed, pigeons that were trained to respond quickly to simple stimuli were more adept using the left eye than the right (DiStefano et al., 1987). Because the stimuli in the study by DiStefano et al. (1987) were presented in the pigeon's frontal binocular field, which is mainly represented in the tectofugal system (Remy and Güntürkün, 1991; Güntürkün and Hahmann, 1999; Budzynski et al., 2002), the shorter latencies of right rotundal bottom-up cells might indeed guide faster visuomotor responses to simple stimuli.

The longer duration of left rotundal activation patterns might indicate a more elaborate stimulus analysis within the left tectofugal system. Because left rotundal lesions have a significantly higher impact on visual accuracy than those on the right (Güntürkün and Hahmann, 1999), and because the right eye of the pigeon is superior in discriminating visual patterns in the frontal visual field (Güntürkün and Kesch, 1987; Güntürkün and Kischkel, 1992; Nottelmann et al., 2002), the longer activity durations of left-rotundal bottom-up neurons might indeed be related to the superiority of the left tectofugal system in processing of various stimulus properties.

Only in the left Rt did we find bottom-up responses from the ipsilateral eye. The left Rt receives more afferents from the contralateral OT than the right Rt, enabling a more bilateral representation within the left tectofugal system (Güntürkün et al., 1998). Therefore, our initial hypothesis predicted a higher proportion of ipsilateral responses in the left Rt. Although the principal pattern of our data are similar to our expectations, only 6.75% ($n = 5$) of all recorded units with bottom-up afferents had an ipsilateral input. Thus, it is possible that the degree of bilateral visual representation within the ascending tectorotundal projec-

tion is a smaller driving force on behavioral visual lateralization than are the asymmetries of top-down control.

All bottom-up asymmetries reached significance, but the effects were not pronounced and should therefore be interpreted with caution. Because the left-right differences of top-down control were striking, it might be possible that the lateralization of the ascending tectofugal system results from secondary plastic changes imposed by top-down descending fibers. Although this possibility cannot be excluded, it probably does not explain all lateralized bottom-up effects. The thalamofugal system matures considerably later than the tectofugal one and is functional only at the time of hatch in chicks (Wu and Karten, 1998; Wu et al., 2000). Although the sequence of ontogenetic effects is comparable in chicks and pigeons, neural ontogenetic maturation speed is slower in the pigeon (Manns and Güntürkün, 1997). Because prehatching light stimulation induces anatomical asymmetries within the mesencephalon and diencephalon of pigeons (Manns and Güntürkün, 1999a,b, 2003), these effects are caused by lateralized changes of the ascending tectofugal system at a time in which top-down effects from the Wulst are possibly not functional. Thus, bottom-up asymmetries are probably not secondary to left-right differences of top-down control.

Top-down asymmetries

We did not find a single left-rotundal neuron with top-down components after ipsilateral stimulation. Likewise, we could not obtain a single right-rotundal top-down component after contralateral stimulation. The most parsimonious explanation for this finding is that unilateral visual stimulation activates a descending pathway that is guided entirely by the left forebrain. Studies involving transections of telencephalotectal fibers support this notion. Whereas right-sided TSM and TOM transections have no impact on visual discriminations, left-sided lesions cause severe disturbances of visually controlled behavior (Güntürkün, 1984; Güntürkün and Hoferichter, 1985).

Within left Rt, most bottom-up and all of the top-down effects are communicated by the right-eye system. This is radically different for the right Rt in which bottom-up input derives from left eye stimulation, whereas all top-down effects originate from right eye input. Thus, bilateral integration predominates at right rotundal level. This pattern might explain behavioral data on complementary specializations of the left-eye and the right-eye system in birds. Avian species are better with their left-eye system in topographical learning tasks that involve relational configurations and positional cues (Rashid and Andrew, 1989; Clayton and Krebs, 1994; Kahn and Bingman, 2004; Vallortigara et al., 2004). Consequently, right hippocampal lesions destroy the ability of chicks to encode global cues of visual information that is scattered across their visual field (Tommasi et al., 2003). It might be possible that the right hemispheric specialization for relational configurations is attributable to the bilateral visual input via bottom-up and top-down sources. In contrast, the left tectofugal system, which mainly receives unilateral input from the contralateral eye via bottom-up and top-down mechanisms, might be specialized to an elaborate analysis of visual patterns seen by the right eye (Rogers, 1996; Güntürkün et al., 2000; Vallortigara et al., 2004). In view of this data, it is conceivable that the asymmetrical modes of processing within the pigeons' tectofugal system outline the neural realization of complementary modes of visual processing.

References

Bagnoli P, Francesconi W, Magni F (1977) Visual Wulst influences on the optic tectum of the pigeon. Brain Behav Evol 14:217–237.

Bagnoli P, Francesconi W, Magni F (1982) Visual Wulst-optic tectum relationships in birds: a comparison with the mammalian corticotectal system. Arch Ital Biol 120:212–235.

Bischof HJ, Niemann J (1990) Contralateral projections of the optic tectum in the zebra finch. Cell Tissue Res 262:307–313.

Britto LR (1978) Hyperstriatal projections to primary visual relays in pigeons: electrophysiological studies. Brain Res 153:382–386.

Budzynski CA, Gagliardo A, Ioale P, Bingman VP (2002) Participation of the homing pigeon thalamofugal visual pathway in sun-compass associative learning. Eur J Neurosci 15:197–210.

Clayton NS, Krebs JR (1994) Memory for spatial and object-specific cues in food-storing and nonstoring birds. J Comp Physiol [A] 174:371–379.

Deng C, Rogers LJ (2002) Prehatching visual experience and lateralization in the visual Wulst of the chick. Behav Brain Res 134:375–385.

DiStefano M, Kusmic C, Musumeci D (1987) Binocular interactions measured by choice reaction times in pigeons. Behav Brain Res 25:161–165.

Dubbeldam JL, den Boer-Visser AM, Bout RG (1997) Organization and efferent connections of the archistriatum of the mallard, *Anas platyrhynchos L.*: an anterograde and retrograde tracing study. J Comp Neurol 388:632–657.

Engelage J, Bischof HJ (1993) The organization of the tectofugal pathway in birds: a comparative review. In: Vision, brain, and behavior in birds (Zeigler HP, Bischof HJ, eds), pp 137–158. Cambridge, MA: MIT.

Fung SH, Burstein D, Born RT (1998) In vivo microelectrode track reconstruction using magnetic resonance imaging. J Neurosci Methods 80:215–224.

Granda AM, Yazulla S (1971) The spectral sensitivity of single units in the nucleus rotundus of pigeon, *Columba livia*. J Gen Physiol 57:363–384.

Green JD (1958) A simple microelectrode for recording from the central nervous system. Nature 182:962.

Güntürkün O (1984) Verhaltensphysiologische Untersuchungen im visuellen System der Taube. PhD thesis, Ruhr-University Bochum.

Güntürkün O (2002) Hemispheric asymmetry in the visual system of birds. In: Brain asymmetry, Ed 2 (Hugdahl K, Davidson RJ, eds), pp 3–36. Cambridge, MA: MIT.

Güntürkün O, Hahmann U (1999) Functional subdivisions of the ascending visual pathways in the pigeon. Behav Brain Res 98:193–201.

Güntürkün O, Hoferichter HH (1985) Neglect after section of a left telencephalotectal tract in pigeons. Behav Brain Res 18:1–9.

Güntürkün O, Kesch S (1987) Visual lateralization during feeding in pigeons. Behav Neurosci 101:433–435.

Güntürkün O, Kischkel KF (1992) Is visual lateralization sex-dependent in pigeons? Behav Brain Res 47:83–87.

Güntürkün O, Miceli D, Watanabe M (1993) Anatomy of the avian thalamofugal pathway. In: Vision, brain, and behavior in birds. (Zeigler HP, Bischof HJ, eds), pp 115–135. Cambridge, MA: MIT.

Güntürkün O, Hellmann B, Melsbach G, Prior H (1998) Asymmetries of representation in the visual system of pigeons. NeuroReport 9:4117–4130.

Güntürkün O, Diekamp B, Manns M, Nottelmann F, Prior H, Schwarz A, Skiba M (2000) Asymmetry pays: visual lateralization improves discrimination success in pigeons. Curr Biol 10:1079–1081.

Gusel'nikov VI, Morenkov ED, Do Kong Khun (1976) Reactions and properties of the receptive fields of neurons in the visual projection zone of the pigeon hyperstriatum. Neirofiziologiia 8:230–236.

Hardy O, Leresche N, Jassik-Gerschenfeld D (1984) Postsynaptic potentials in neurons of the pigeon's optic tectum in response to afferent stimulation from the retina and other visual structures: an intracellular study. Brain Res 311:65–74.

Husband SA, Shimizu T (1999) Efferent projections of the ectostriatum in the pigeon (*Columba livia*). J Comp Neurol 406:329–345.

Kahn MC, Bingman VP (2004) Lateralization of spatial learning in the avian hippocampal formation. Behav Neurosci 118:333–344.

Karten HJ, Hodos W (1967) A stereotaxic atlas of the brain of the pigeon. Baltimore: Johns Hopkins UP.

Karten HJ, Cox K, Mpodozis J (1997) Two distinct populations of tectal neurons have unique connections within the retinotectorotundal pathway of the pigeon (*Columba livia*). J Comp Neurol 387:449–465.

Koshiba M, Nakamura S, Deng C, Rogers LJ (2003) Light-dependent development of asymmetry in the ipsilateral and contralateral thalamofugal visual projections of the chick. Neurosci Lett 336:81–84.

Leresche N, Hardy O, Jassik-Gerschenfeld D (1983) Receptive field properties of single cells in the pigeon's optic tectum during cooling of the "visual Wulst." Brain Res 267:225–236.

Letelier JC, Mpodozis J, Marin G, Morales D, Rozas C, Madrid C, Velasco M (2000) Spatiotemporal profile of synaptic activation produced by the electrical and visual stimulation of retinal inputs to the optic tectum: a current source density analysis in the pigeon (*Columba livia*). Eur J Neurosci 12:47–57.

Manns M, Güntürkün O (1997) Development of the retinotectal system in the pigeon: a choleratoxin study. Anat Embryol (Berl) 195:539–555.

Manns M, Güntürkün O (1999a) 'Natural' and artificial monocular deprivation effects on thalamic soma sizes in pigeons. NeuroReport 10:3223–3228.

Manns M, Güntürkün O (1999b) Monocular deprivation alters the direction of functional and morphological asymmetries in the pigeon's visual system. Behav Neurosci 113:1–10.

Manns M, Güntürkün O (2003) Light experience induces differential asymmetry patterns of GABA- and parvalbumine-positive cells in the pigeon's visual midbrain. J Chem Neuroanat 25:249–259.

Martin JH (1991) Autoradiographic estimation of the extent of reversible inactivation produced by microinjection of lidocaine and muscimol in the rat. Neurosci Lett 127:160–164.

Miceli D, Reperant J, Villalobos J, Dionne L (1987) Extratelencephalic projections of the avian visual Wulst. A quantitative autoradiographic study in the pigeon (*Columbia livia*). J Hirnforsch 28:45–57.

Mpodozis J, Cox K, Shimizu T, Bischof HJ, Woodson W, Karten HJ (1996) GABAergic inputs to the nucleus rotundus (pulvinar inferior) of the pigeon (*Columba livia*). J Comp Neurol 374:204–222.

Nottelmann F, Wohlschläger A, Güntürkün O (2002) Unihemispheric memory in pigeons-knowledge, the left hemisphere is reluctant to share. Behav Brain Res 133:309–315.

Perisic M, Mihailovic J, Cuenod M (1971) Electrophysiology of contralateral and ipsilateral visual projections to the Wulst in pigeon (*Columba livia*). Int J Neurosci 2:7–14.

Rashid N, Andrew RJ (1989) Right hemisphere advantage for topographic orientation in the domestic chick. Neuropsychologia 27:937–948.

Reiner A, Perkel DJ, Bruce LL, Butler AB, Csillag A, Kuenzel W, Medina L, Paxinos G, Shimizu T, Striedter G, Wild M, Ball GF, Durand S, Güntürkün O, Lee DW, Mello CV, Powers A, White SA, Hough G, Kubikova L, Smulders TV, Wada K, Dugas-Ford J, Husband S, Yamamoto K, Yu J, Siang C, Jarvis ED (2004) Revised nomenclature for avian telencephalon and some related brainstem nuclei. J Comp Neurol 473:377–414.

Remy M, Güntürkün O (1991) Retinal afferents to the tectum opticum and the nucleus opticus principalis thalami in the pigeon. J Comp Neurol 305:57–70.

Revzin AM (1970) Some characteristics of wide-field units in the brain of the pigeon. Brain Behav Evol 3:195–204.

Robert F, Cuénod M (1969) Electrophysiology of the intertectal commissures in the pigeon. II. Inhibitory interaction. Exp Brain Res 9:123–136.

Rogers LJ (1996) Behavioral, structural and neurochemical asymmetries in the avian brain: a model system for studying visual development and processing. Neurosci Biobehav Rev 20:487–503.

Rogers LJ, Andrew RJ (2002) Introduction. In: Comparative vertebrate lateralization (Rogers LJ, Andrew RJ, eds), pp 1–5. Cambridge, UK: Cambridge UP.

Rushton WA (1951) A theory of the effects of fiber size in medullated nerve. J Physiol (Lond) 115:101–122.

Saleh CN, Ehrlich D (1984) Composition of the supraoptic decussation of the chick (*Gallus gallus*). A possible factor limiting interhemispheric transfer of visual information. Cell Tissue Res 236:601–609.

Sandkühler J, Maisch B, Zimmermann M (1987) The use of local anaesthetic microinjections to identify central pathways: a quantitative evaluation of the time course and extent of the neuronal block. Exp Brain Res 68:168–178.

Schmidt A, Bischof HJ (2001) Integration of information from both eyes by single neurons of nucleus rotundus, ectostriatum and lateral neostriatum in the zebra finch (*Taeniopygia guttata castanotis Gould*). Brain Res 923:20–31.

Shimizu T, Karten HJ (1993) The avian visual system and the evolution of the neocortex. In: Vision, brain, and behavior in birds (Zeigler HP, Bischof HJ, eds), pp 104–114. Cambridge, MA: MIT.

Shimizu T, Cox K, Karten HJ (1995) Intratelencephalic projections of the visual Wulst in pigeons (*Columba livia*). J Comp Neurol 359:551–572.

Sun H, Frost BJ (1998) Computation of different optical variables of looming objects in pigeon nucleus rotundus neurons. Nat Neurosci 1:296–303.

Theiss MP, Hellmann B, Güntürkün O (2003) The architecture of an inhibitory sidepath within the avian tectofugal system. NeuroReport 14:879–882.

Tommasi L, Gagliardo A, Andrew RJ, Vallortigara G (2003) Seperate processing mechanisms for encoding of geometric and landmark information in the avian hippocampus. Eur J Neurosci 17:1695–1702.

Vallortigara G, Pagni P, Sovrano VA (2004) Separate geometric and non-geometric modules for spatial reorientation: evidence from a lopsided animal brain. J Cogn Neurosci 16:390–400.

Voss J, Bischof HJ (2003) Regulation of ipsilateral visual information within the tectofugal visual system in zebra finches. J Comp Physiol A Neuroethol Sens Neural Behav Physiol 189:545–553.

Wang YC, Jiang S, Frost BJ (1993) Visual processing in pigeon nucleus rotundus: luminance, color, motion, and looming subdivisions. Vis Neurosci 10:21–30.

Webster KE (1974) Changing concepts of the organization of the central visual pathways in birds. In: Essays on the nervous system (Bellairs R, Gray EG, eds), pp 259–297. Oxford: Clarendon.

Wu CC, Karten HJ (1998) The thalamo-hyperstriatal system is established by the time of hatching in chicks (*Gallus gallus*): a cholera toxin B subunit study. Vis Neurosci 15:349–358.

Wu CC, Charlton RK, Karten HJ (2000) The timecourse of neuronal connections of the rotundoectostriatal pathway in chicks (*Gallus gallus*) during embryogenesis: a retrograde transport study. Vis Neurosci 17:905–909.

Yano J (1976) The EEG response to repetitive photic stimulation in various regions of the chicken brain. Electroencephalogr Clin Neurophysiol 40:244–252.

Zeier H, Karten HJ (1971) The archistriatum of the pigeon: organization of afferent and efferent connections. Brain Res 31:313–326.